Geophysical Research Letters

RESEARCH LETTER
10.1029/2019GL084088

Indian Ocean Warming Trend Reduces Pacific Warming Response to Anthropogenic Greenhouse Gases: An Interbasin Thermostat Mechanism

Lei Zhang[1], Weiqing Han[1], Kristopher B. Karnauskas[1,2], Gerald A. Meehl[3], Aixue Hu[3], Nan Rosenbloom[3], and Toshiaki Shinoda[4]

[1]Department of Atmospheric and Oceanic Sciences, University of Colorado Boulder, Boulder, CO, USA, [2]Cooperative Institute for Research in Environmental Sciences, Boulder, CO, USA, [3]National Center for Atmospheric Research, Boulder, CO, USA, [4]Department of Physical and Environmental Sciences, Texas A&M University-Corpus Christi, Corpus Christi, TX, USA

Key Points:
- The interbasin warming contrast is a robust observational feature, which is not present in climate models
- The Indian Ocean warming effectively reduces the Pacific warming response to anthropogenic greenhouse gases
- The reason that climate models fail to capture the interbasin warming contrast is likely due to model bias

Supporting Information:
- Supporting Information S1

Correspondence to:
L. Zhang,
lezh8230@colorado.edu

Citation:
Zhang, L., Han, W., Karnauskas, K. B., Meehl, G. A., Hu, A., Rosenbloom, N., & Shinoda, T. (2019). Indian Ocean warming trend reduces Pacific warming response to anthropogenic greenhouse gases: An interbasin thermostat mechanism. *Geophysical Research Letters*, *46*, 10,882–10,890. https://doi.org/10.1029/2019GL084088

Received 13 JUN 2019
Accepted 2 SEP 2019
Accepted article online 6 SEP 2019
Published online 15 OCT 2019

Abstract A greater warming trend of sea surface temperature in the tropical Indian Ocean than in the tropical Pacific is a robust feature found in various observational data sets. Yet this interbasin warming contrast is not present in climate models. Here we investigate the impact of tropical Indian Ocean warming on the tropical Pacific response to anthropogenic greenhouse gas warming by analyzing results from coupled model pacemaker experiments. We find that warming in the Indian Ocean induces local negative sea level pressure anomalies, which extend to the western tropical Pacific, strengthening the zonal sea level pressure gradient and easterly trades in the tropical Pacific. The enhanced trade winds reduce sea surface temperature in the eastern tropical Pacific by increasing equatorial upwelling and evaporative cooling, which offset the greenhouse gas warming. This result suggests an interbasin thermostat mechanism, through which the Indian Ocean exerts its influence on the Pacific response to anthropogenic greenhouse gas warming.

1. Introduction

Variability of the atmosphere-ocean coupled system in the tropical Indo-Pacific region has prominent impacts on global climate (Alexander et al., 2002; Hoskins & Karoly, 1981; Wallace & Gutzler, 1981). Understanding how the tropical Pacific responds to anthropogenic greenhouse gas (GHG) warming is therefore of paramount importance for future climate prediction and climate change adaptation (Clement et al., 1996; Knutson & Manabe, 1995; Knutson & Manabe, 1998; Seager & Vecchi, 2010; Vecchi et al., 2006; Xie et al., 2010).

The majority of climate models that participated in the Coupled Model Intercomparison Project phase 5 (CMIP5) simulated an El Niño-like sea surface temperature (SST) warming pattern in response to GHG forcing, with a larger warming appearing in the eastern tropical Pacific relative to the western tropical Pacific (Figure 1d; Held & Soden, 2006; Vecchi & Soden, 2007b; Xie et al., 2010; Zhang & Li, 2014). The long-term SST trends in observational data sets, however, exhibit different patterns from those in the CMIP5 models (Coats & Karnauskas, 2017; Zhang, 2016; Zhang et al., 2018). While some observational data sets show a weak La Niña-like SST trend pattern with a small negative SST trend in the eastern tropical Pacific (Figures 1a and 1b), others show negligible changes in the zonal SST gradient (Figures 1c and S1; Solomon & Newman, 2012). The differences among the observational data sets may result from the sparsity of observations in the early twentieth century (Deser et al., 2010; Vecchi et al., 2006). The distinct model-data and cross-data differences have led to an intense debate on whether there will be an El Niño-like or a La Niña-like SST trend pattern under global warming (Clement et al., 1996; Compo & Sardeshmukh, 2010; Karnauskas et al., 2009; Knutson & Manabe, 1995; Seager & Murtugudde, 1997; Vecchi et al., 2006; Vecchi & Soden, 2007b; Xie et al., 2010; Zhang & Karnauskas, 2017; Zhang & Li, 2014).

Various physical mechanisms have been proposed to explain the formation of the El Niño-like SST warming in CMIP5 models, that is, larger evaporative damping in the warm pool than the cold tongue (Knutson & Manabe, 1995; Xie et al., 2010; Zhang & Li, 2014), different cloud feedback in the western and eastern tropical Pacific due to different cloud regimes (DiNezio et al., 2009; Meehl & Washington, 1996; Zhang & Li, 2014), weakening of the Pacific Walker circulation due to enhanced tropospheric static stability (Knutson &

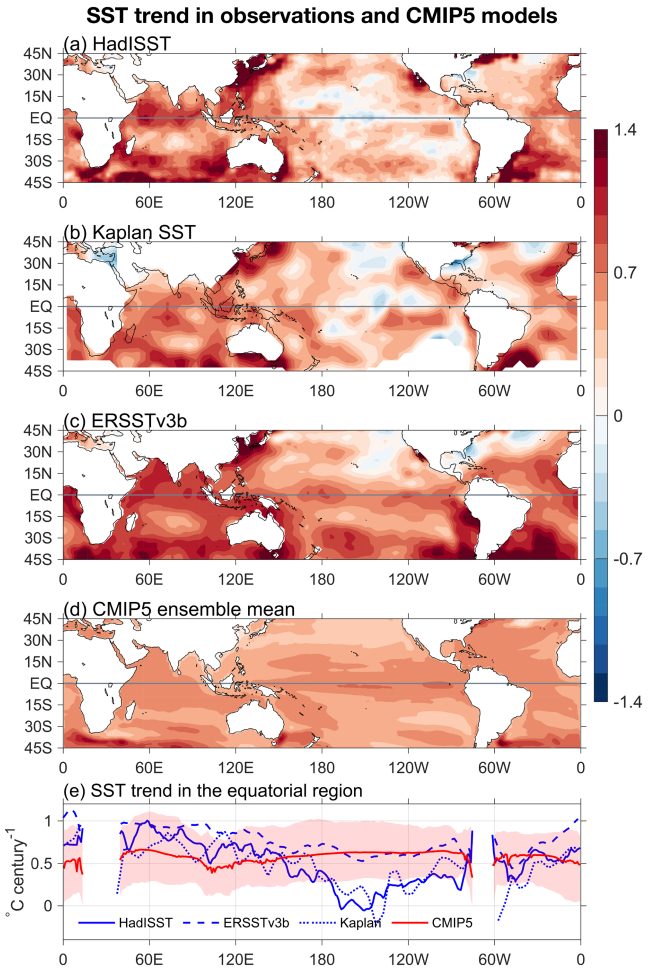

Figure 1. SST trend over the period 1920–2013 in observations and CMIP5 climate models. Units are °C/century. (a–c) Results for HadISST, Kaplan SST, and ERSSTv3b, respectively. (d) Ensemble mean of CMIP5 results (1920–2013). (e) SST trend averaged between 10°N and 10°S. Solid blue for HadISST, dashed blue for ERSSTv3b, dotted blue for Kaplan SST, and solid red for CMIP5 results. Red shading denotes the intermodel spread of SST warming trend, defined as 10th and 90th percentile, for CMIP5 results.

Manabe, 1995; Ma et al., 2012) and/or the slowdown of global hydrologic cycle (Held & Soden, 2006; Vecchi & Soden, 2007b), and larger land-ocean thermal contrast (Bayr & Dommenget, 2013; Zhang & Li, 2017). On the other hand, Clement et al. (1996) analyzed Pacific changes under GHG warming using an intermediate-complexity Cane and Zebiak-type model (Zebiak & Cane, 1987) and found a La Niña-like SST response. They attributed the eastern Pacific cooling anomalies to ocean dynamical cooling effect associated with enhanced upper ocean stratification and the strong upwelling of the mean state (the "ocean dynamical thermostat mechanism"). These results were later reproduced by Seager and Murtugudde (1997) using a more complex oceanic general circulation model. Hence, the tropical Pacific SST response to GHG warming remains controversial and thus demands further investigation.

Note that the aforementioned studies have focused on the ocean-atmosphere coupling processes within the tropical Pacific basin. Recent studies, however, have shown that variability of the tropical Indian Ocean has prominent impacts on the tropical Pacific at both interannual (Annamalai et al., 2005; Xie et al., 2009) and decadal time scales (Han et al., 2014; Luo et al., 2012; Luo et al., 2018; Zhang et al., 2018). Yet the possible role of the tropical Indian Ocean in modulating the tropical Pacific response to anthropogenic warming remains unclear. Despite the significant uncertainties in the Pacific SST warming trend among different SST data sets, all of the observed SST data show a larger SST warming in the tropical Indian Ocean than in the tropical Pacific (Figure 1), suggesting that the signal of an interbasin warming contrast is robust to cross-data set differences. Zhang et al. (2019) formulated a simple box model to investigate this problem and found that the Indian Ocean warming reduces the Pacific warming response to the GHG effect. Using atmospheric general circulation model (AGCM) experiments, Zhang and Karnauskas (2017) showed that the Indian Ocean warming trend strengthens the Pacific trade winds (also see Luo et al., 2012; Han et al., 2014); the response of tropical Pacific SST to the enhanced easterly trades, however, could not be examined by the standalone AGCM experiments. In this study, we analyze the results from a suite of experiments using coupled global climate models, to assess the role of the tropical Indian Ocean warming in causing Pacific SST anomalies (SSTA) under global warming.

2. Experimental Design

To investigate the impact of tropical Indian Ocean SST warming on the tropical Pacific under global warming, a 10-member ensemble of Indian Ocean-Global Atmosphere (IOGA) pacemaker experiments (see Kosaka and Xie (2013) for a description of the pacemaker methodology applied to the tropical Pacific) is conducted using the National Center for Atmospheric Research (NCAR) Community Earth System Model version 1 (CESM1; Hurrell et al., 2013). Each ensemble member has slightly different initial conditions. In all IOGA pacemaker experiments, SST in the tropical Indian Ocean and part of the western Pacific warm pool region is restored to observed values from National Oceanic and Atmospheric Administration Extended Reconstructed SST version 3b (ERSSTv3b; Figure 2a). A sponge layer is utilized in the northern, southern, and eastern boundaries of the restoring region. The rest of the global ocean is freely coupled to the atmosphere. External forcing (both anthropogenic and natural) applied in IOGA is the same as that in CMIP5 historical simulations (1920–2005) and Representative Concentration Pathway version 8.5 (2006–2013). Therefore, the ensemble mean of the IOGA experiments isolates the effects of both Indian Ocean warming and external forcing. The IOGA experiments have been recently analyzed to explore the impact of the tropical Indian Ocean forcing in affecting the midlatitude jet (Yang et al., 2019; personal communication).

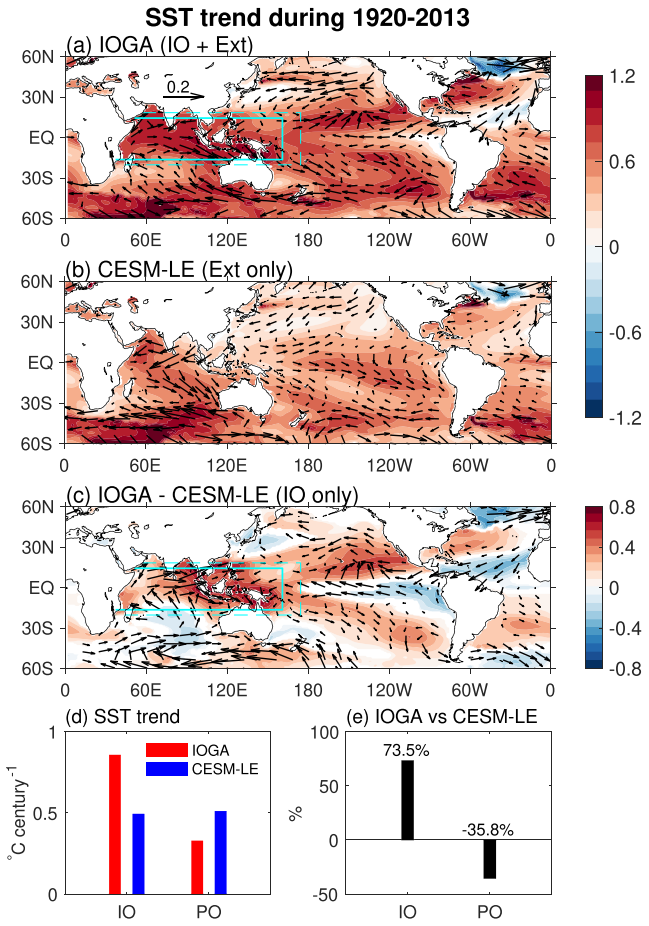

Figure 2. Trends of SST (°C/century) and surface wind stress (dyn cm^{-2} $century^{-1}$) over the period 1920–2013 in the ensemble mean of IOGA (SST in the Indian Ocean is restored to observations in addition to prescribed external forcing, "IO + ext"), and CESM-LE with external forcing only ("ext only"). The solid line in (a) (approximately 28°E–161°E and 16°S–14.5°N) indicates where SSTs are restored to observations, and the area between the solid and dashed lines denote the sponge layer. (a and b) Results for IOGA and CESM-LE, respectively. (c) Differences between IOGA and CESM-LE (IOGA–CESM-LE) which, by subtracting out the external forcing in the CESM-LE, leaves only the influence of the Indian Ocean SSTs ("IO only"). Shading and vectors in (a)–(c) denote results that are statistically significant at 90% confidence level based on two-sided Student's *t* test. (d) SST trend (°C/century) averaged over the tropical Indian Ocean (15°N–15°S, 60°E–120°E) and eastern equatorial Pacific (5°N–5°S, 150°W–80°W). Red for IOGA and blue for CESM-LE. (e) Percentage differences of SST trend (%) between IOGA and CESM-LE. First column shows result for the tropical Indian Ocean, and second column shows result for the eastern equatorial Pacific.

Since we focus on the impact of the tropical Indian Ocean SSTA on the tropical Pacific, we further analyze the CESM Large-Ensemble (CESM-LE; Kay et al., 2015) experiments to extract the effects of the external forcing. CESM-LE has 40 members with roundoff level perturbation added onto the initial atmospheric temperature conditions. Since internal variability is not synchronized across different ensemble members, the ensemble average can filter out internal variability and primarily represent the effect of the external forcing. Therefore, the differences between the ensemble means of the two sets of experiments result mainly from the effects of additional Indian Ocean SST warming in observations compared to CESM-LE (Figure 2). Whether or not the different magnitudes of Indian Ocean SST warming between climate models and observational data sets result from natural climate variability will be addressed later. Note that the model configuration and external forcing applied in IOGA and CESM-LE are identical. The only exception is the ozone forcing. While CESM-LE used Whole Atmosphere Community Climate Model (Marsh et al., 2013) ozone, IOGA was forced by Stratosphere-Troposphere Processes and Their Role in Climate (Eyring et al., 2013) ozone data. This difference in external forcing causes statistically indistinguishable differences in simulated tropical climate in CESM (e.g., Schneider et al., 2015), and therefore has minimal influence on the results discussed here.

Observational SST data sets used in this study are from the Hadley Centre Sea Ice and SST (HadISST; Rayner et al., 2003), the ERSST (version 3b (Smith et al., 2008), version 4 (Huang et al., 2015), and version 5 (Huang et al., 2017)), and the Kaplan SST (Kaplan et al., 1998). The analysis period is 1920–2013, the same as the simulation period of the numerical experiments described above. SSTA is obtained by removing the monthly climatology during 1920–2013. Due to sparse observations during the early twentieth century, the 1920–2013 trend of the atmospheric circulation exhibits large spread across different atmospheric reanalysis data sets (DiNezio et al., 2013). Hence, we mainly rely on model experiments to examine changes in the Pacific Walker circulation under global warming, although we used wind data from National Oceanic and Atmospheric Administration twentieth-century reanalysis version 2c (Compo et al., 2011) to analyze its mean state distribution. As a comparison, we also analyze the SST trend patterns for 1920–2013 from the historical simulations and the Representative Concentration Pathway version 8.5 experiments of 32 CMIP5 models (Table S1 and Figure 1d).

3. Results

Despite the uncertainties over the Pacific across different data sets due to the different methodologies used to derive these gridded data sets, all observational data sets exhibit a prominent warming trend in the tropical Indian Ocean, which clearly outpaces the warming rate of the tropical Pacific, although this interbasin warming contrast is smaller in ERSSTv3b than that in HadISST and Kaplan SST (Figure 1). This result is different from the CMIP5 model results, which show a similar (or smaller) magnitude of warming in the tropical Indian Ocean as (than) that in the tropical Pacific. This interbasin warming contrast between tropical Indian and Pacific Oceans is robust to uncertainties across different observed data sets, but it is totally missing in the climate model simulations.

To assess the impacts of the Indian Ocean warming and the external forcing on the Pacific SSTA, we analyze the ensemble means of IOGA and CESM-LE experiments. Note that although part of the observed SST warming in the western tropical Pacific is included in IOGA, the maximum warming in the region is mainly located in the tropical Indian Ocean (Figure 2a). Under the influences of both Indian Ocean warming and

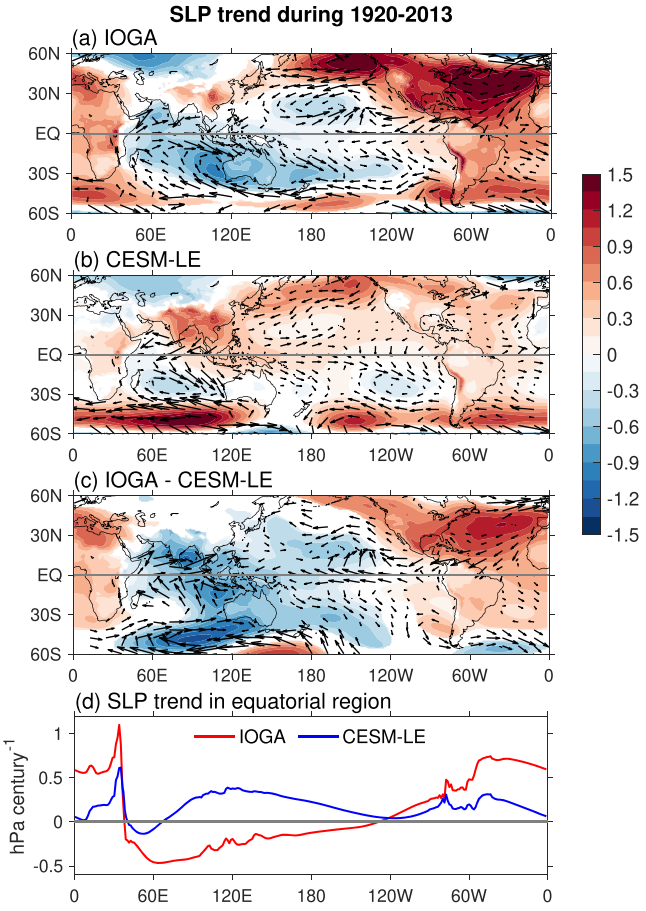

Figure 3. (a–c) Same as Figures 2a–2c but for SLP trend (hPa/century). Shading and vectors denote results that are statistically significant at 90% confidence level based on two-sided Student's *t* test. (d) SLP trend averaged between 5°N and 5°S. Red shows IOGA results, and blue shows CESM-LE results.

GHG forcing, the Pacific zonal SST gradient increases in IOGA, with a larger (smaller) SST warming in the western (eastern) tropical Pacific. Correspondingly, easterly wind anomalies appear over the tropical Pacific, suggesting an enhanced Pacific Walker circulation (Figure S2). The enhanced Pacific zonal SST gradient in the IOGA pacemaker experiment is different from the SST trend pattern in ERSSTv3b, but consistent with HadISST and Kaplan SST results, although the IOGA experiments were forced by ERSSTv3b which has the weakest interbasin warming contrast. The discrepancies among different observational SST data sets are likely due to the sparse and thus less-reliable SST observations during early twentieth century.

The IOGA results are different from those in the CESM-LE and CMIP5 results, which simulate an El Niño-like warming accompanied by a weakened Walker circulation in the tropical Pacific region (Figures 2b and 1d). In the tropical Indian Ocean, easterly wind anomalies and a larger (smaller) SST warming in the western (eastern) Indian Ocean appear in CESM-LE, which are consistent with the bias identified in CMIP models (Annamalai et al., 2017; Gent et al., 2011; Zhang & Li, 2014). Corresponding to the opposite changes in the tropical Pacific SST and winds between IOGA and CESM-LE, precipitation changes in the two experiments are also opposite (Figure S3).

These differences between IOGA and CESM-LE highlight the important role of the tropical Indian Ocean warming in affecting change in the Pacific (Figure 2c), and this effect is underestimated by the conventional climate models. In response to the additional tropical Indian Ocean SST warming in IOGA relative to CESM-LE, pronounced strengthening of the easterly wind occupies the entire tropical Pacific, together with eastern Pacific cooling anomalies. The tropical Indian Ocean is dominated by westerly wind anomalies, which are likely a Rossby wave response to the basin-wide SST warming and the associated positive precipitation anomalies (Gill, 1980). Overall, the observed Indian Ocean SST warming is ~73.5% larger than that in CESM-LE, which induces ~35.8% reduction of warming in the eastern tropical Pacific in IOGA compared to CESM-LE (Figures 2d and 2e). A recent study by Luo et al. (2018) also found that climate models tend to underestimate the interbasin warming contrast since the 1980s, which could contribute to the simulated El Niño-like SST warming pattern in recent decades.

How does the Indian Ocean warming affect the Pacific air-sea coupled system? As found in Zhang and Karnauskas (2017), the additional warming in the tropical Indian Ocean relative to the tropical Pacific enhances the Pacific easterly trades through an atmospheric bridge. Indeed, IOGA results show that warming in the Indian Ocean induces basin-wide negative sea level pressure (SLP) anomalies, which extend to the western tropical Pacific as a Kelvin wave response (Figures 3a and 3c). Convective heating due to positive precipitation anomalies associated with the tropical Indian Ocean warming likely also contributes to the negative SLP anomalies in IOGA (Figure S3a; Gill, 1980). As a result, the zonal SLP gradient over the tropical Pacific is enhanced compared to the mean state, inducing strengthened Pacific easterly winds (Figure 3d). The agreement between previous AGCM results that are forced by tropical Indian Ocean SST warming trend (e.g.Han et al., 2014, Luo et al., 2012, Zhang & Karnauskas, 2017) and IOGA results further supports that change in the Pacific between IOGA and CESM-LE is primarily due to the Indian Ocean effect, although part of the western tropical Pacific warming is included in IOGA experiments. By contrast, CESM-LE simulates positive SLP and negative precipitation anomalies in the Indo-Pacific warm pool region in response to the external forcing, which then drive westerly wind anomalies over the tropical Pacific (Figures 3b and 3d), favoring the El Niño-like SST warming. It is also noted that there is a significant connection to the Atlantic as well, with positive SLP anomalies there associated with the SST forcing in the Indian Ocean (Figure 3c), which could also contribute to the strengthening of the Pacific Walker circulation. Previous

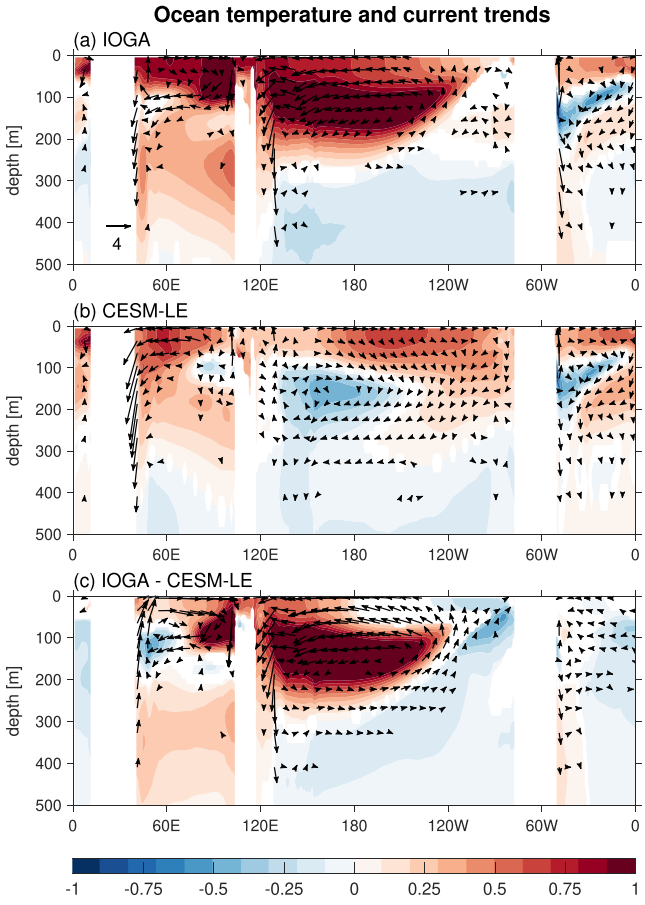

Figure 4. (a–c) Same as Figures 2a–2c but for trends of ocean temperature (°C/century), zonal (cm s^{-1} $century^{-1}$), and vertical currents (10^{-5} cm s^{-1} $century^{-1}$).

studies have indeed shown close interbasin connections for the tropical Atlantic-Indian Ocean (Li et al., 2016) and tropical Atlantic-Pacific (England et al., 2014; Taschetto et al., 2015).

In IOGA, the enhanced Pacific easterly trades further cause Pacific cooling anomalies (Figure 2c). Through strengthening the equatorial Ekman divergence, the anomalous easterly trades enhance oceanic upwelling and thus cause SST cooling in the eastern tropical Pacific, which partly offsets the anthropogenic warming effect (Figures 4a and 4c). In addition, the surface westward ocean current anomalies driven by the easterly wind anomalies increase the transport of the cold water from the eastern basin to the central tropical Pacific. In the western tropical Pacific, enhanced oceanic downwelling contributes to the prominent subsurface warming anomalies. Consistently, negative (positive) sea level anomalies show up in the eastern (western) tropical Pacific, suggesting shallower (deeper) thermocline depth (Figures S4d and S4f). In addition to the ocean dynamical effect, increased surface wind speeds over the tropical Pacific cause larger surface latent heat loss and thereby further cool down the ocean surface (Figures S4 and S5). This effect, however, is confined in the central equatorial Pacific, while in the eastern equatorial Pacific, the surface latent heat flux trend is positive (less surface latent heat loss), which is due to lower SST in situ. In the tropical Indian Ocean, westerly wind anomalies drive eastward surface ocean current anomalies, piling up the warm water in the eastern tropical Indian Ocean. Upper ocean current and temperature anomalies as well as sea level anomalies and surface wind speed anomalies in the tropical Indian and Pacific Oceans exhibit opposite changes in CESM-LE compared to IOGA (Figures 4 and S4).

The above results clearly show that the interbasin warming contrast, that is, the greater warming in the Indian Ocean than in the tropical Pacific, plays an important role in causing Pacific changes under global warming, but this effect is not well simulated by climate models. These model-data discrepancies could be due to the model biases in simulating the Indian Ocean warming, and/or influences of natural internal climate variability. To further shed light on this issue, we compare observational results with those from each member of the CESM-LE and CMIP5 models. Note that differences among different ensemble members of CESM-LE are solely due to influences of internal variability, while the spread of the CMIP5 model results is associated with both internal variability and differences in model physics and structure. We find that the interbasin warming contrast in the three observational data sets is well above the 90th percentile of that in CESM-LE and CMIP5 models (Figure 5a). The slightly negative mean and median values in climate models suggest that the simulated Indian Ocean warming is actually smaller than that in the tropical Pacific. These results suggest that the model-data differences of the interbasin warming contrast cannot be explained by influences of internal variability, and thus could be primarily attributable to model biases in simulating external forced signals. It is worth mentioning that the above comparisons have not fully taken into account the model biases in simulating natural internal climate variability; weaker-than-observed internal variability in climate models would lead to underestimation of their impacts on the centennial trend and the small model spread in Figure 5, which might contribute partly to the model-data differences.

The warming trends in the tropical Indian and Pacific Oceans are further shown separately and compared against each other in Figure 5b. The different interbasin warming contrast across different ensemble members of CESM-LE is mainly due to variations in the simulated Pacific Ocean warming trend, which is due to the influence of the Interdecadal Pacific Oscillation (IPO). The spread of the Indian Ocean warming in CESM-LE is much smaller, indicating that the anthropogenic warming trend dominates its relatively weak decadal variability (Zhang et al., 2018). By contrast, in the CMIP5 models, magnitudes of the warming trends in the two ocean basins are tightly linked, with a large (small) Indian Ocean warming corresponding to a large (small) Pacific Ocean warming, which may be related to different model sensitivities to the

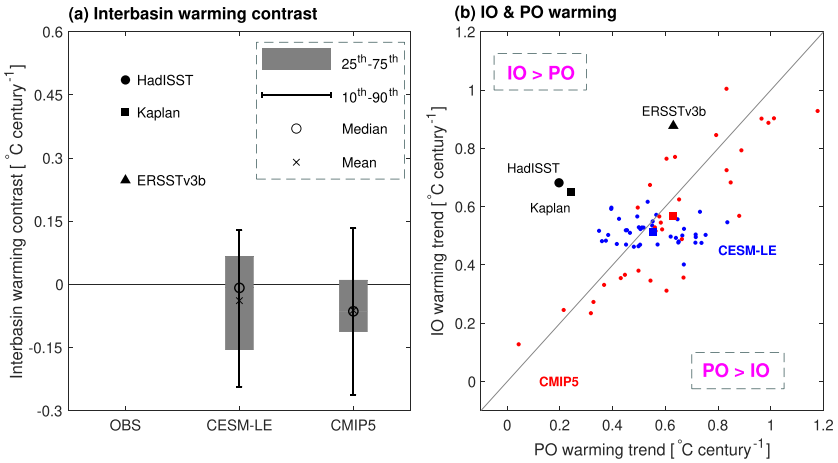

Figure 5. (a) Differences between tropical Indian Ocean warming trend (50°E–120°E, 20°N–20°S) and eastern tropical Pacific warming trend (180°–90°W, 10°N–10°S). Positive values mean greater Indian Ocean warming trend than that in the eastern tropical Pacific. First column shows results from observational SST data sets. Circle, square, and triangle denote results from HadISST, Kaplan, and ERSSTv3b, respectively. Results using ERSSTv4 and ERSSTv5 are similar to ERSSTv3b and thus are not shown. Second column shows the percentiles of the interbasin warming contrast in CESM-LE. Third column is the same as the second column, but for CMIP5 results. Hollow circle and cross sign in second and third columns denote the median and mean values. Gray bars and vertical lines denote 25th–75th and 10th–90th percentiles. (b) Scatterplot of Pacific Ocean warming trend against Indian Ocean warming trend. Black circle, square, and triangle denote HadISST, Kaplan, and ERSSTv3b results. Blue (red) dots denote CESM-LE (CMIP5) results.

anthropogenic GHG forcing. None of the CMIP5 models or CESM-LE can simulate an interbasin warming contrast as large as that in observations.

4. Summary and Discussion

The spatial pattern of the centennial (1920–2013) SST warming trend in the tropical Pacific under influences of anthropogenic forcing is still uncertain due to the cross-data and model-data differences. In spite of these uncertainties, we find a robust signal of interbasin warming contrast from observations, with a larger rate of SST warming in the tropical Indian Ocean than that in the tropical Pacific. This interbasin warming contrast, however, is not captured by climate model simulations. By analyzing the ensemble mean of IOGA pacemaker experiments and the CESM-LE, we isolate and compare the impacts of tropical Indian Ocean warming and external forcing on Pacific SST and Walker circulation under global warming.

The ensemble average of the CESM-LE, which measures the effect of external forcing, shows an El Niño-like SST warming in the tropical Pacific with an underestimated Indian Ocean warming rate. Instead of a faster Indian Ocean warming, the model produces similar warming magnitudes in the tropical Indian and Pacific Oceans. This result is consistent with the ensemble mean of CMIP5 models. In IOGA, which measures the effects of external forcing plus realistic Indian Ocean warming, the tropical Indian Ocean warming rate outpaces that in CESM-LE, introducing an interbasin warming contrast in the tropical Indo-Pacific region. The prominent tropical Indian Ocean warming induces negative SLP anomalies that extend eastward to the western tropical Pacific, which enhance the Pacific zonal SLP gradient and drive easterly wind anomalies. The strengthened Pacific easterly trades enhance the oceanic upwelling, westward zonal currents, and latent heat loss to the atmosphere, cooling the SST in the central and eastern tropical Pacific. Positive SLP anomalies in the Atlantic Ocean due to the Indian Ocean forcing may also contribute to the strengthening of the Pacific Walker circulation.

Note that it is the interbasin warming contrast, that is, the additional Indian Ocean warming relative to the tropical Pacific, that enables the tropical Indian Ocean to actively affect the tropical Pacific. This is because SLP anomalies are essentially a form of mass redistribution, and hence, it is the relative SST warming (compared to the tropical mean warming), instead of the absolute SST warming, that is directly applicable to inferring SLP anomalies, which are critical in driving large-scale wind anomalies. Such an argument is similar to

the so-called "warmer-get-wetter" mechanism (Xie et al., 2010) and the dependence of changes of hurricane activity on the relative SST warming (Latif et al., 2007; Lee et al., 2011; Vecchi et al., 2008; Vecchi & Soden, 2007a). Assuming a smaller warming rate in the tropical Indian Ocean than the tropical Pacific under global warming, one would expect that the tropical Indian Ocean changes would be dominated by the remote Pacific forcing, which seems to be the case in climate models.

One important question is what causes the smaller warming rate of the tropical Pacific than the tropical Indian Ocean initially, which allows the latter to further suppress the warming response in the former region via the interbasin atmospheric bridge, maintaining or amplifying the interbasin warming contrast. One plausible hypothesis is the "ocean dynamical thermostat mechanism" (Clement et al., 1996; Sun & Liu, 1996). The strong and persistent upper ocean upwelling in the eastern equatorial Pacific damps the surface warming caused by the anthropogenic GHG forcing, leading to a smaller warming rate in the tropical Pacific. In the tropical Indian Ocean, the mean oceanic upwelling zone is located in the southwest tropical basin off the equator, and therefore, the equatorial Indian Ocean SST increases faster than that in the tropical Pacific under global warming, resulting in an interbasin warming contrast. Subsequently, the greater Indian Ocean warming further reduces the Pacific positive SSTA. Hence, this is an *interbasin thermostat mechanism*.

We further compare interbasin warming differences in observations with those in individual ensemble members of CESM-LE and CMIP5 models and find that the observed values are well above the range of simulated ones. This result suggests that the model-data differences may not be due to the influences of internal variability, but may be mainly caused by model biases, such as model biases in local air-sea interaction processes in the tropical Pacific (Luo et al., 2018), and/or misrepresentation of the eastern equatorial Pacific circulation and coupling (Coats & Karnauskas, 2018), both of which may lead to too weak ocean dynamical cooling effect. Biases in the Indian Ocean mean states (SST is too high in the west) and associated biases in precipitation and winds also likely contribute to model-data differences in the pattern and magnitude of the Indian Ocean warming trend (Annamalai et al., 2017; Gent et al., 2011). The other possibility is that because the Pacific cold tongue extends too far west in climate models, the simulated Pacific easterly trades are overly strong, which may yield too strong influences from the Pacific to the Indian Ocean. Indeed, it is found that the biases in the cold tongue and zonal winds are reduced in the IOGA experiments compared to the CESM-LE, thanks to the realistic Indian Ocean SST forcing in the former (Figure S6).

The comparisons between observations and climate models, however, have not fully taken into account the discrepancies of internal climate variabilities between them. Previous studies have at least partly attributed the SST cooling trend in the tropical Pacific since the late 1990s to the negative phase of the IPO (England et al., 2014; Kosaka & Xie, 2013; Zhang, 2016), yet the IPO amplitude is generally underestimated by CMIP5 models (Kociuba & Power, 2014). Therefore, the significant model-data differences of the interbasin warming contrast could be partly associated with model biases in simulating the natural internal climate variabilities. Given the prominent role of the tropical Indian Ocean warming in contributing to Pacific changes under global warming, it is important to explore in detail the causes for the large discrepancies in the Indian Ocean warming magnitude between observations and climate models, and a future study targeting the relative roles of external forcing and internal climate variability in causing the interbasin warming contrast is warranted.

Acknowledgments
ERSST and Kaplan SST are provided by NOAA/OAR/ESRL PSD, Boulder, CO, USA, from their Web site. HadISST data set is obtained from https://www.metoffice.gov.uk/hadobs/hadisst/. The 20CRv2c data are from https://www.esrl.noaa.gov/psd/data/gridded/data.20thC_ReanV2c.html. CESM-LE outputs are downloaded from http://www.cesm.ucar.edu/projects/community-projects/LENS/. IOGA pacemaker experiments presented in this study are available at http://atoc.colorado.edu/~whan/. Portions of this study were supported by National Science Foundation (NSF) AGS 1446480, the Regional and Global Model Analysis (RGMA) component of the Earth and Environmental System Modeling Program of the U.S. Department of Energy's Office of Biological & Environmental Research (BER) via NSF IA 1844590. The National Center for Atmospheric Research is sponsored by the NSF. T.S. is also supported by NSF grant OCE-1658218, NASA grant NNX17AH25G, and NOAA grants NA15OAR431074 and NA17OAR4310256.

References

Alexander, M. A., Bladé, I., Newman, M., Lanzante, J. R., Lau, N.-C., & Scott, J. D. (2002). The atmospheric bridge: The influence of ENSO teleconnections on air–sea interaction over the global oceans. *Journal of Climate*, *15*(16), 2205–2231. https://doi.org/10.1175/1520-0442(2002)015<2205:TABTIO>2.0.CO;2

Annamalai, H., Taguchi, B., McCreary, J. P., Nagura, M., & Miyama, T. (2017). Systematic errors in South Asian monsoon simulation: Importance of equatorial Indian Ocean processes. *Journal of Climate*, *30*(20), 8159–8178. https://doi.org/10.1175/JCLI-D-16-0573.1

Annamalai, H., Xie, S. P., McCreary, J. P., & Murtugudde, R. (2005). Impact of Indian Ocean sea surface temperature on developing El Niño*. *Journal of Climate*, *18*(2), 302–319. https://doi.org/10.1175/JCLI-3268.1

Bayr, T., & Dommenget, D. (2013). The tropospheric land–sea warming contrast as the driver of tropical sea level pressure changes. *Journal of Climate*, *26*(4), 1387–1402. https://doi.org/10.1175/JCLI-D-11-00731.1

Clement, A. C., Seager, R., Cane, M. A., & Zebiak, S. E. (1996). An ocean dynamical thermostat. *Journal of Climate*, *9*(9), 2190–2196. https://doi.org/10.1175/1520-0442(1996)009<2190:AODT>2.0.CO;2

Coats, S., & Karnauskas, K. B. (2017). Are simulated and observed twentieth century tropical Pacific sea surface temperature trends significant relative to internal variability? *Geophysical Research Letters*, *44*, 9928–9937. https://doi.org/10.1002/2017GL074622

Coats, S., & Karnauskas, K. B. (2018). A role for the equatorial undercurrent in the ocean dynamical thermostat. *Journal of Climate*, *31*(16), 6245–6261. https://doi.org/10.1175/JCLI-D-17-0513.1

Compo, G. P., & Sardeshmukh, P. D. (2010). Removing ENSO-related variations from the climate record. *Journal of Climate*, *23*(8), 1957–1978. https://doi.org/10.1175/2009JCLI2735.1

Compo, G. P., Whitaker, J. S., Sardeshmukh, P. D., Matsui, N., Allan, R. J., Yin, X., et al. (2011). The Twentieth Century Reanalysis Project. *Quarterly Journal of the Royal Meteorological Society*, *137*(654), 1–28. https://doi.org/10.1002/qj.776

Deser, C., Phillips, A. S., & Alexander, M. A. (2010). Twentieth century tropical sea surface temperature trends revisited. *Geophysical Research Letters*, *37*, L10701. https://doi.org/10.1029/2010GL043321

DiNezio, P. N., Clement, A. C., Vecchi, G. A., Soden, B. J., Kirtman, B. P., & Lee, S.-K. (2009). Climate response of the equatorial Pacific to global warming. *Journal of Climate*, *22*(18), 4873–4892. https://doi.org/10.1175/2009JCLI2982.1

DiNezio, P. N., Vecchi, G. A., & Clement, A. C. (2013). Detectability of changes in the Walker circulation in response to global warming*. *Journal of Climate*, *26*(12), 4038–4048. https://doi.org/10.1175/JCLI-D-12-00531.1

England, M. H., McGregor, S., Spence, P., Meehl, G. A., Timmermann, A., Cai, W., et al. (2014). Recent intensification of wind-driven circulation in the Pacific and the ongoing warming hiatus. *Nature Climate Change*, *4*(3), 222–227. https://doi.org/10.1038/nclimate2106

Eyring, V., Arblaster, J. M., Cionni, I., Sedláček, J., Perlwitz, J., Young, P. J., et al. (2013). Long-term ozone changes and associated climate impacts in CMIP5 simulations. *Journal of Geophysical Research: Atmospheres*, *118*, 5029–5060. https://doi.org/10.1002/jgrd.50316

Gent, P. R., Danabasoglu, G., Donner, L. J., Holland, M. M., Hunke, E. C., Jayne, S. R., et al. (2011). The Community Climate System Model version 4. *Journal of Climate*, *24*(19), 4973–4991. https://doi.org/10.1175/2011JCLI4083.1

Gill, A. E. (1980). Some simple solutions for heat-induced tropical circulation. *Quarterly Journal of the Royal Meteorological Society*, *106*(449), 447–462. https://doi.org/10.1002/qj.49710644905

Han, W., Meehl, G. A., Hu, A., Alexander, M. A., Yamagata, T., Yuan, D., et al. (2014). Intensification of decadal and multi-decadal sea level variability in the western tropical Pacific during recent decades. *Climate Dynamics*, *43*(5-6), 1357–1379. https://doi.org/10.1007/s00382-013-1951-1

Held, I. M., & Soden, B. J. (2006). Robust responses of the hydrological cycle to global warming. *Journal of Climate*, *19*(21), 5686–5699. https://doi.org/10.1175/JCLI3990.1

Hoskins, B. J., & Karoly, D. J. (1981). The steady linear response of a spherical atmosphere to thermal and orographic forcing. *Journal of the Atmospheric Sciences*, *38*(6), 1179–1196. https://doi.org/10.1175/1520-0469(1981)038<1179:TSLROA>2.0.CO;2

Huang, B., Banzon, V. F., Freeman, E., Lawrimore, J., Liu, W., Peterson, T. C., et al. (2015). Extended Reconstructed Sea Surface Temperature version 4 (ERSST.v4). Part I: Upgrades and intercomparisons. *Journal of Climate*, *28*(3), 911–930. https://doi.org/10.1175/JCLI-D-14-00006.1

Huang, B., Thorne, P. W., Banzon, V. F., Boyer, T., Chepurin, G., Lawrimore, J. H., et al. (2017). Extended Reconstructed Sea Surface Temperature, version 5 (ERSSTv5): Upgrades, validations, and intercomparisons. *Journal of Climate*, *30*(20), 8179–8205. https://doi.org/10.1175/JCLI-D-16-0836.1

Hurrell, J. W., Holland, M. M., Gent, P. R., Ghan, S., Kay, J. E., Kushner, P. J., et al. (2013). The Community Earth System Model: A framework for collaborative research. *Bulletin of the American Meteorological Society*, *94*(9), 1339–1360. https://doi.org/10.1175/BAMS-D-12-00121.1

Kaplan, A., Cane, M. A., Kushnir, Y., Clement, A. C., Blumenthal, M. B., & Rajagopalan, B. (1998). Analyses of global sea surface temperature 1856–1991. *Journal of Geophysical Research*, *103*(C9), 18,567–18,589. https://doi.org/10.1029/97JC01736

Karnauskas, K. B., Seager, R., Kaplan, A., Kushnir, Y., & Cane, M. A. (2009). Observed strengthening of the zonal sea surface temperature gradient across the equatorial Pacific Ocean*. *Journal of Climate*, *22*(16), 4316–4321. https://doi.org/10.1175/2009JCLI2936.1

Kay, J. E., Deser, C., Phillips, A., Mai, A., Hannay, C., Strand, G., et al. (2015). The Community Earth System Model (CESM) Large Ensemble Project: A community resource for studying climate change in the presence of internal climate variability. *Bulletin of the American Meteorological Society*, *96*(8), 1333–1349. https://doi.org/10.1175/BAMS-D-13-00255.1

Knutson, T. R., & Manabe, S. (1995). Time-mean response over the tropical Pacific to increased CO_2 in a coupled ocean-atmosphere model. *Journal of Climate*, *8*(9), 2181–2199. https://doi.org/10.1175/1520-0442(1995)008<2181:TMROTT>2.0.CO;2

Knutson, T. R., & Manabe, S. (1998). Model assessment of decadal variability and trends in the tropical Pacific Ocean. *Journal of Climate*, *11*(9), 2273–2296. https://doi.org/10.1175/1520-0442(1998)011<2273:MAODVA>2.0.CO;2

Kociuba, G., & Power, S. B. (2014). Inability of CMIP5 models to simulate recent strengthening of the Walker circulation: Implications for projections. *Journal of Climate*, *28*(1), 20–35. https://doi.org/10.1175/JCLI-D-13-00752.1

Kosaka, Y., & Xie, S.-P. (2013). Recent global-warming hiatus tied to equatorial Pacific surface cooling. *Nature*, *501*(7467), 403–407. https://doi.org/10.1038/nature12534

Latif, M., Keenlyside, N., & Bader, J. (2007). Tropical sea surface temperature, vertical wind shear, and hurricane development. *Geophysical Research Letters*, *34*, L01710. https://doi.org/10.1029/2006GL027969

Lee, S.-K., Enfield, D. B., & Wang, C. (2011). Future impact of differential interbasin ocean warming on Atlantic hurricanes. *Journal of Climate*, *24*(4), 1264–1275. https://doi.org/10.1175/2010JCLI3883.1

Li, X., Xie, S.-P., Gille, S. T., & Yoo, C. (2016). Atlantic-induced pan-tropical climate change over the past three decades. *Nature Climate Change*, *6*(3), 275–279. https://doi.org/10.1038/nclimate2840

Luo, J.-J., Sasaki, W., & Masumoto, Y. (2012). Indian Ocean warming modulates Pacific climate change. *Proceedings of the National Academy of Sciences of the United States of America*, *109*(46), 18,701–18,706. https://doi.org/10.1073/pnas.1210239109

Luo, J.-J., Wang, G., & Dommenget, D. (2018). May common model biases reduce CMIP5's ability to simulate the recent Pacific La Niña-like cooling? *Climate Dynamics*, *50*(3-4), 1335–1351. https://doi.org/10.1007/s00382-017-3688-8

Ma, J., Xie, S.-P., & Kosaka, Y. (2012). Mechanisms for tropical tropospheric circulation change in response to global warming*. *Journal of Climate*, *25*(8), 2979–2994. https://doi.org/10.1175/JCLI-D-11-00048.1

Marsh, D. R., Mills, M. J., Kinnison, D. E., Lamarque, J., Calvo, N., & Polvani, L. M. (2013). Climate change from 1850 to 2005 simulated in CESM1 (WACCM). *Journal of Climate*, *26*(19), 7372–7391. https://doi.org/10.1175/JCLI-D-12-00558.1

Meehl, G. A., & Washington, W. M. (1996). El Niño-like climate change in a model with increased atmospheric CO_2 concentrations. *Nature*, *382*(6586), 56–60. https://doi.org/10.1038/382056a0

Rayner, N. A., Parker, D. E., Horton, E. B., Folland, C. K., Alexander, L. V., Rowell, D. P., et al. (2003). Global analyses of sea surface temperature, sea ice, and night marine air temperature since the late nineteenth century. *Journal of Geophysical Research*, *108*(D14), 4407. https://doi.org/10.1029/2002JD002670

Schneider, D. P., Deser, C., & Fan, T. (2015). Comparing the impacts of tropical SST variability and polar stratospheric ozone loss on the Southern Ocean westerly winds*. *Journal of Climate*, *28*(23), 9350–9372. https://doi.org/10.1175/JCLI-D-15-0090.1

Seager, R., & Murtugudde, R. (1997). Ocean dynamics, thermocline adjustment, and regulation of tropical SST. *Journal of Climate*, *10*(3), 521–534. https://doi.org/10.1175/1520-0442(1997)010<0521:ODTAAR>2.0.CO;2

Seager, R., & Vecchi, G. A. (2010). Greenhouse warming and the 21st century hydroclimate of southwestern North America. *Proceedings of the National Academy of Sciences of the United States of America*, *107*(50), 21,277–21,282. https://doi.org/10.1073/pnas.0910856107

Smith, T. M., Reynolds, R. W., Peterson, T. C., & Lawrimore, J. (2008). Improvements to NOAA's historical merged land–ocean surface temperature analysis (1880–2006). *Journal of Climate*, *21*(10), 2283–2296. https://doi.org/10.1175/2007JCLI2100.1

Solomon, A., & Newman, M. (2012). Reconciling disparate twentieth-century Indo-Pacific ocean temperature trends in the instrumental record. *Nature Climate Change*, *2*(9), 691–699. https://doi.org/10.1038/nclimate1591

Sun, D.-Z., & Liu, Z. (1996). Dynamic ocean-atmosphere coupling: A thermostat for the tropics. *Science*, *272*(5265), 1148–1150. https://doi.org/10.1126/science.272.5265.1148

Taschetto, A. S., Rodrigues, R. R., Meehl, G. A., McGregor, S., & England, M. H. (2015). How sensitive are the Pacific–tropical North Atlantic teleconnections to the position and intensity of El Niño-related warming? *Climate Dynamics*, *46*(5-6), 1841–1860. https://doi.org/10.1007/s00382-015-2679-x

Vecchi, G. A., & Soden, B. J. (2007a). Effect of remote sea surface temperature change on tropical cyclone potential intensity. *Nature*, *450*(7172), 1066–1070. https://doi.org/10.1038/nature06423

Vecchi, G. A., & Soden, B. J. (2007b). Global warming and the weakening of the tropical circulation. *Journal of Climate*, *20*(17), 4316–4340. https://doi.org/10.1175/JCLI4258.1

Vecchi, G. A., Soden, B. J., Wittenberg, A. T., Held, I. M., Leetmaa, A., & Harrison, M. J. (2006). Weakening of tropical Pacific atmospheric circulation due to anthropogenic forcing. *Nature*, *441*(7089), 73–76. https://doi.org/10.1038/nature04744

Vecchi, G. A., Swanson, K. L., & Soden, B. J. (2008). Climate change: Whither hurricane activity? *Science*, *322*(5902), 687–689. https://doi.org/10.1126/science.1164396

Wallace, J. M., & Gutzler, D. S. (1981). Teleconnections in the geopotential height field during the Northern Hemisphere winter. *Monthly Weather Review*, *109*(4), 784–812. https://doi.org/10.1175/1520-0493(1981)109<0784:TITGHF>2.0.CO;2

Xie, S.-P., Deser, C., Vecchi, G. A., Ma, J., Teng, H., & Wittenberg, A. T. (2010). Global warming pattern formation: Sea surface temperature and rainfall*. *Journal of Climate*, *23*(4), 966–986. https://doi.org/10.1175/2009JCLI3329.1

Xie, S.-P., Hu, K., Hafner, J., Tokinaga, H., Du, Y., Huang, G., & Sampe, T. (2009). Indian Ocean capacitor effect on Indo–Western Pacific climate during the summer following El Niño. *Journal of Climate*, *22*(3), 730–747. https://doi.org/10.1175/2008JCLI2544.1

Yang, D., Arblaster, J. M., Meehl, G. A., England, M., Bates, S., Rosenbloom, N., & Lim, E.-P. (2019). What drives the decadal shift of the Southern Hemisphere eddy-driven jet? *Journal of Climate*.

Zebiak, S. E., & Cane, M. A. (1987). A model El Niño–Southern Oscillation. *Monthly Weather Review*, *115*(10), 2262–2278. https://doi.org/10.1175/1520-0493(1987)115<2262:AMENO>2.0.CO;2

Zhang, L. (2016). The roles of external forcing and natural variability in global warming hiatuses. *Climate Dynamics*, *47*(9-10), 3157–3169. https://doi.org/10.1007/s00382-016-3018-6

Zhang, L., Han, W., & Sienz, F. (2018). Unraveling causes for the changing behavior of tropical Indian Ocean in the past few decades. *Journal of Climate*, *31*(6), 2377–2388. https://doi.org/10.1175/JCLI-D-17-0445.1

Zhang, L., & Karnauskas, K. B. (2017). The role of tropical interbasin SST gradients in forcing Walker circulation trends. *Journal of Climate*, *30*(2), 499–508. https://doi.org/10.1175/JCLI-D-16-0349.1

Zhang, L., & Li, T. (2014). A simple analytical model for understanding the formation of sea surface temperature patterns under global warming. *Journal of Climate*, *27*(22), 8413–8421. https://doi.org/10.1175/JCLI-D-14-00346.1

Zhang, L., & Li, T. (2017). Relative roles of differential SST warming, uniform SST warming and land surface warming in determining the Walker circulation changes under global warming. *Climate Dynamics*, *48*(3-4), 987–997. https://doi.org/10.1007/s00382-016-3123-6

Zhang, L., Sun, D.-Z., & Karnauskas, K. B. (2019). The role of the Indian Ocean in determining the tropical Pacific SST response to radiative forcing in an idealized model. *Dynamics of Atmospheres and Oceans*, *86*, 1–9. https://doi.org/10.1016/j.dynatmoce.2019.02.003